materials

MDPI

Article

The Impact of TPA Auxiliary Donor and the π-Linkers on the Performance of Newly Designed Dye-Sensitized Solar Cells: Computational Investigation

Si Mohamed Bouzzine [1,2,*], Alioui Abdelaaziz [2], Mohamed Hamidi [2], Fatimah A. M. Al-Zahrani [3], Mohie E. M. Zayed [4] and Reda M. El-Shishtawy [4,5,*]

[1] Regional Center for Education and Training Professional, B.P. 8 Errachidia, Morocco
[2] Equipe de Chimie-Physique, Electrochimie et Environnement, Laboratoire de Chimie-Physique, Environnement et Matériaux, Université Moulay Ismaïl, B.P. 509 Boutalamine, Errachidia, Morocco
[3] Chemistry Department, Faculty of Science, King Khalid University, P.O. Box 9004, Abha 61413, Saudi Arabia
[4] Chemistry Department, Faculty of Science, King Abdulaziz University, Jeddah 21589, Saudi Arabia
[5] Dyeing, Printing and Textile Auxiliaries Department, Textile Research and Technology Institute, National Research Centre, 33 EL Buhouth St., Dokki, Giza 12622, Egypt
* Correspondence: mbouzzine@yahoo.fr (S.M.B.); relshishtawy@kau.edu.sa (R.M.E.-S.)

Abstract: The efficiency of the newly designed dye-sensitized solar cells (DSSCs) containing triphenylamine, diphenylamine (TPA), phenothiazine, and phenoxazine as donors and triazine, phenyl with D_1-D_2-π-linker-π-$(A)_2$ architecture has been investigated using density functional theory (DFT) and time-dependent (TD-DFT) methods. These methods were used to investigate the geometrical structures, electronic properties, absorption, photovoltaic properties, and chemical reactivity. Furthermore, the calculated results indicate that different architectures can modify the energy levels of HOMO and LUMO and reduce the energy gap. The absorption undergoes a redshift displacement. This work aims at calculating the structural geometries and the electronic and optical properties of the designed dyes. Furthermore, the dye adsorption characteristics, such as the optoelectronic properties and the adsorption energies in the TiO_2 clusters, were calculated with counterpoise correction and discussed.

Keywords: dye-sensitized solar cells; di-anchoring; TD/TD-DFT; D_1-D_2-π-linker-π-$(A)_2$; photovoltaic properties

Citation: Bouzzine, S.M.; Abdelaaziz, A.; Hamidi, M.; Al-Zahrani, F.A.M.; Zayed, M.E.M.; El-Shishtawy, R.M. The Impact of TPA Auxiliary Donor and the π-Linkers on the Performance of Newly Designed Dye-Sensitized Solar Cells: Computational Investigation. *Materials* **2023**, *16*, 1611. https://doi.org/10.3390/ma16041611

Academic Editor: Ana Belen Munoz Garcia

Received: 10 November 2022
Revised: 20 December 2022
Accepted: 10 February 2023
Published: 15 February 2023

1. Introduction

An increase in the world population and the increasing consumption of fossils and the more severe environmental pollution crisis contribute immensely to high-energy demand. In addition, growing world energy demand and limited oil and coal reserves will limit future economic development. It is, therefore, necessary to exploit renewable energy sources, such as solar energy, to maintain sustainable social and economic development. Solar energy is widely recognized as the most promising candidate for helping solve this problem. In this interest, the search for an efficient method for harnessing solar light conversion to electricity using dyes-sensitized solar cells (DSSCs) has been investigated [1–7]. The solution-processable photovoltaic DSSCs have the advantages of being clean, cheap, renewable, inexhaustible, pollution-free, and large-scale production [8–14]. Because of their lower production cost, DSSCs offer a viable alternative to conventional all-inorganic solar cells. Over the past decades, DSSCs have attracted a great deal of attention as an alternative to silicon solar cells because they use environmentally friendly materials through inexpensive processes and offer commercially feasible energy conversion efficiency [15–17].

Numerous attempts at molecular modification based on dyes characteristic of D-π-A have been carried out to improve the photoelectric performance of DSSC devices. There are many new dyes with new designs, such as D-π-A, whose theoretical study was interested in the performance of photovoltaic properties [18–20]. Sometimes we find dyes where we

have double donor D-D-π-A or double acceptor D-A-π-A or double π-spacer D-π-A-π-D [21–24]. S. Gauthier et al. synthesized di-anchoring type D-$(\pi\text{-A})_2$ dyes with a PEC of 5.23% [25], whereas M. B. Desta et al. studied three new D-$(\pi\text{-A})_2$ di-anchoring organic dyes comprising an arylamine as the electron donor with a maximum of PEC 6.69% [26]. Other types of dyes, L(D-π-$A)_2$ di-anchoring organic, were investigated by Z. Wang et al. [27].

This new dye design, which could enhance the D-π-A concept, emphasized the possibility that ordinary organic dyes' single anchor group would be a drawback in comparison to dyes containing up to four anchor groups [28–30]. As a result, the multi-anchoring dye concept was put forth for the conventional D-π-A architectural design. The interest in this design strategy is justified for a number of reasons. The two bridges in the more complex system should primarily result in an expansion of the absorption at longer wavelengths, a broader absorption profile, and an increased molar extinction coefficient when compared to those of D-A, all of which improve light harvesting. Another electron withdrawing unit (A) might also help improve the organic dye's photostability by lowering its HOMO-LUMO divergence [31].

The present contribution aims to explore better the D_1-D_2-π-linker-π-$(A)_2$ structures (Figure 1) by studying the effects of the change of donor (triphenylamine or diphenylamine) and (phenothiazine or phenoxazine), as well as the impact of pi-linkers (phenyl or triazine) on the geometric and optoelectronic properties of the studied dyes that contain the cyanoacrylic acid group as acceptors, via furan spacers, using density functional theory (DFT) and time-dependent DFT (TD-DFT).

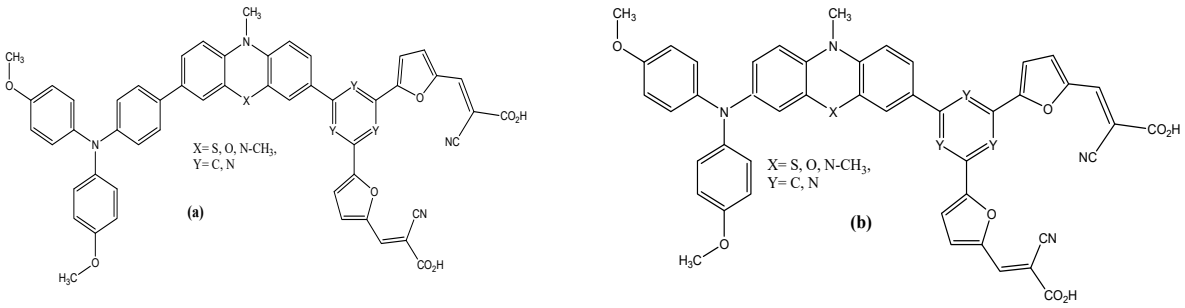

Figure 1. Chemical structures of the designed D_1-D_2-π-linker-π-$(A)_2$ sensitizers (**a**) with triphenylamine (**b**) with diphenylamine.

2. Computational Methods

All calculations were carried out using the Gaussian 09 program package [32]. According to our previous study [33,34], in which the efficiency and robustness of various hybrid and meta-hybrid functional, such as B3LYP [35,36] and BHandH [37], are used in conjunction with their basis-set 6-31G(d,p) for non-metal atoms and LANL2DZ for Ti atoms [38–40] for simulating the geometrical and electronic properties and absorption spectra. The BHandH [37] optimizes the ground state geometry without any symmetry constraint, while the functional BHandH (which includes a fraction of 50% HF exchange) is used to record the UV-vis absorption spectra using a Poples large basis-set 6-31G(d,p) for the soft atoms (H, C, N, O, S) and effective core potential LANL2DZ basis set for titanium atoms [41]. The geometrical optimizations and the absorption spectrum simulations were performed in the chloroform medium using the implicit CPCM [42] model (conductor-like polarizable continuum model). The complexation energy of the Dye@TiO_2 clusters is calculated with the corrected counterpoise method [43], taking into account the Basis set superposition errors (BSSEs) [44,45].

3. Results and Discussion

3.1. Geometrical Properties

As we know, the efficient process of electron transfer and the electronic and optical properties are better with the coplanarity of the geometrical structure of colorants [46]. The

structure optimizations of the studied dyes were performed using the B3LYP/6-31G(d, p) method [36], and the selected geometrical parameters, bond lengths, and dihedral angles are listed in Figure 2 and Table 1. According to the obtained results (Table 1), we can deduce that the θ values, which are the dihedral angles between the acceptor unit (A) and the π-bridge unit (π), are in order 37, 57°, and 35,4°, respectively, for dyes based triphenylamine and diphenylamine using phenyl as a bridge. The observed non-planar structures for all dyes are likely the result of steric effects between the hydrogen of phenyl (π-spacer) and phenothiazine or phenoxazine of the adjacent group, which would contribute to the suppression of dye aggregation problems and charge recombination [47,48]. On the other hand, the dihedral angles θ of dyes bridged by triazine are coplanar. Therefore, the nature of the bridging group has a minor impact on the π-bridge fragment flatness, which will facilitate electron delocalization and thus improve the intramolecular charge transfer and photovoltaic properties of the DSSC [49]. In addition, the values of the distances d_i(i = 1 − 2) of all dyes are in the range of 1.410−1.481 Å. These values are lower than the C-C single bonds (∼1.530 Å) [49], which confirms the strong resonance between the donor and acceptor for all dyes.

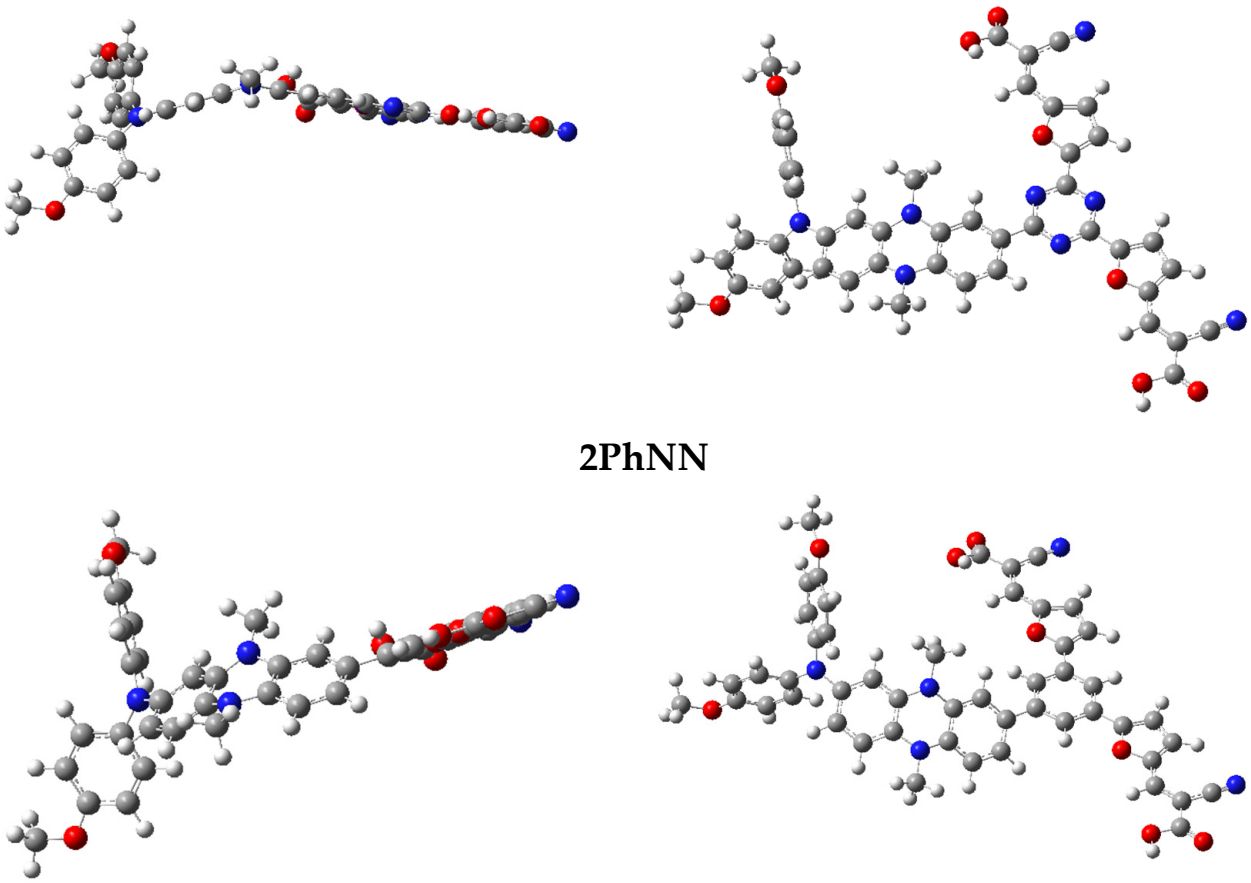

Figure 2. Optimized geometry of 2PhNN and 2PhNC (the other structure is inserted in Figure S1).

Table 1. Values of dihedral angle (θ (°)) and bond length (Å) obtained by B3LYP/6-31G(d,p).

Dyes	d_1(Å)	d_2(Å)	θ (°)	Dyes	d_1(Å)	d_2(Å)	θ (°)
2PhNC	1.415	1.481	36.66	TPhNC	1.481	1.482	37.37
2PhOC	1.411	1.481	35.30	TPhOC	1.481	1.481	36.39
2PhSC	1.410	1.482	34.30	TPhSC	1.480	1.482	35.97
2PhNN	1.414	1.460	0.76	TPhNN	1.480	1.460	0.08
2PhON	1.407	1.462	0.04	TPhON	1.481	1.462	0.05
2PhSN	1.409	1.465	0.20	TPhSN	1.480	1.465	0.07

3.2. Electronic Properties

Using B3LYP/6-31G, the energy gap E_{gap} for the study dyes was calculated from the discrepancies in HOMO and LUMO energy levels (d,p). Table 2a,b contain the results without any restrictions, and the optimization was carried out in the gas phase. The calculated values of orbital HOMO in the studied dyes are between −4.61 eV to −4.88 eV for the first series and between −4.64 eV to −4.97 eV for the second series (Table 2a,b). The energy of the LUMO orbitals has an average of about −3.20 eV for the phenyl-mediated compounds. Whereas, for triphenyl and diphenyl dyes, compounds containing triazine rings show a value of −3.33 eV and −3.42 eV, respectively. The previous results show that the gap value decreases for the same dyes upon replacing phenyl rings with triazine rings. This can only be due to the effect of substituting carbon with nitrogen (phenyl to triazine).

Table 2. a: Values of orbital molecular HOMO, LUMO, and gap energies calculated with B3LYP/6-31G(d,p) level for the studied donor-like triphenylamine-based dyes. **b:** Values of orbital molecular HOMO, LUMO, and gap energies calculated with B3LYP/6-31G(d,p) level for the studied donor-like diphenylamine-based dyes.

(a)				
Dyes		E_{LUMO} (eV)	E_{HOMO} (eV)	E_{gap} (eV)
TPhNC	X = S.O.N Y = C	−3.20	−4.76	1.56
TPhOC		−3.19	−4.88	1.69
TPhSC		−3.12	−4.72	1.60
TPhNN	X = S.O.N Y = N	−3.33	−4.61	1.28
TPhON		−3.35	−4.67	1.32
TPhSN		−3.38	−4.72	1.34
(b)				
Dyes		E_{LUMO} (eV)	E_{HOMO} (eV)	E_{gap} (eV)
2PhNC	X = S.O.N Y = C	−3.20	−4.92	1.72
2PhOC		−3.19	−4.80	1.61
2PhSC		−3.20	−4.64	1.44
2PhNN	X = S.O.N Y = N	−3.42	−4.71	1.29
2PhON		−3.42	−4.88	1.46
2PhSN		−3.46	−4.97	1.51

Differently, TPhOC, 2PhNC, 2PhSN, and 2PhON chromophores' estimated level of HOMO energies are more negative than those of other dyes, while their LUMO values are more positive than those of the TiO_2 conduction band (Figure 3). On the other hand, the HOMO values of these dyes are lower than the $E(I^-/I_3^-)$ redox potential. These HOMO positions indicate that the oxidized form the reduced species in the electrolyte to investigate efficient charge separation. Furthermore, this regeneration was affected by the nature of

the donor and the π-spacers block. This result indicates that these dyes can regenerate the charge and thus can be used in dye-sensitized solar cells.

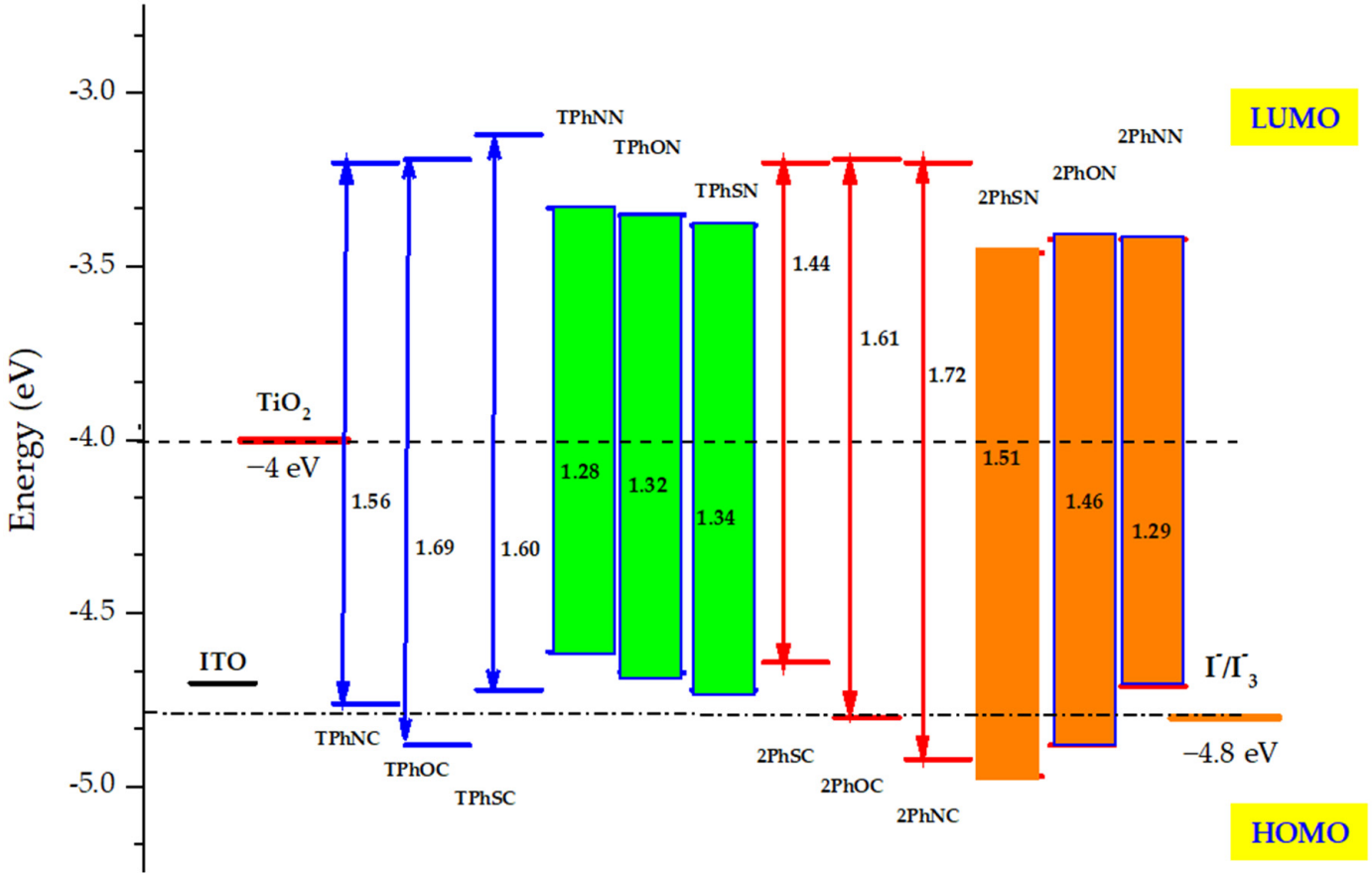

Figure 3. Frontier molecular orbital energy levels and HOMO-LUMO bandgap of all isolated dyes calculated at B3LYP/6-31G (d, p) level, along with the energy of TiO_2 conduction band and the redox potential of I^-/I_3^- electrolyte.

Figure 4a,b, in which the electronic density of the HOMO of all compounds is primarily distributed on the donor (D1 = frag1 and D2 = frag2; see Figure S2). Figure 4a, with high electron density, shows the distribution of the electronic density, as indicated by the HOMO and LUMO orbitals, respectively, which contributed to the electron transition. While in the π-linker and the acceptor (π-linker-π-$(A)_2$), there is a lack of density in the neighboring rings, which is checked by calculating the density contribution (Figure 5a,b). In contrast, the electronic density of the LUMO orbital is mainly displaced at the acceptor and the π-spacer segment (frag3-frag4-frag5-frag6-frag7) (Figure S2). This explains very well the transfer of load from the donor to the acceptor through the spacer.

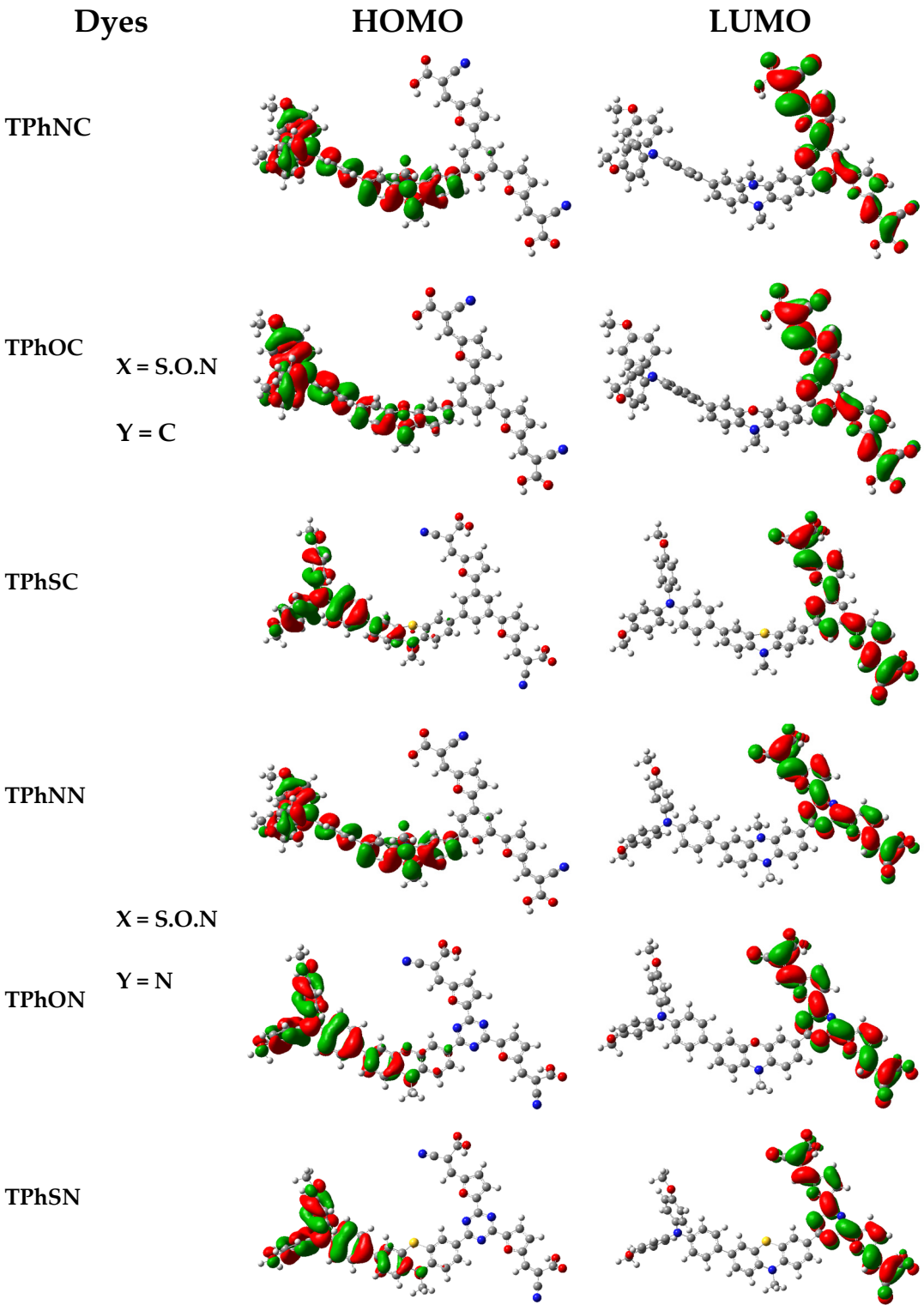

(**a**)

Figure 4. *Cont.*

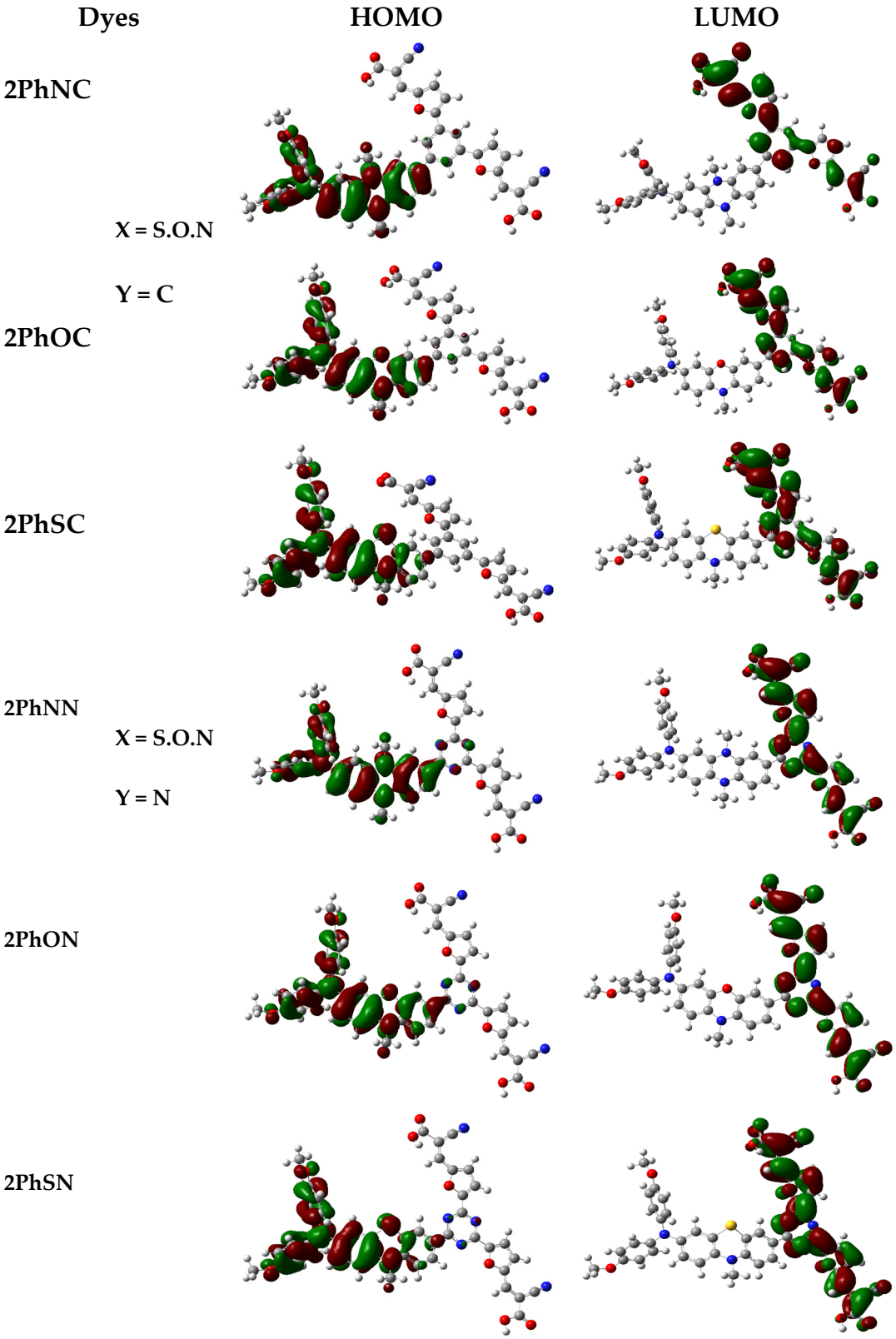

(**b**)

Figure 4. (**a**) Frontier Molecular Orbitals (FMOs) of dyes-based triphenyl amine (TPh) using B3LYP/6-31G(d,p). (**b**): Frontier Molecular Oritals of dyes-based diphenyl amine (2Ph) using B3LYP/6-31G(d,p).

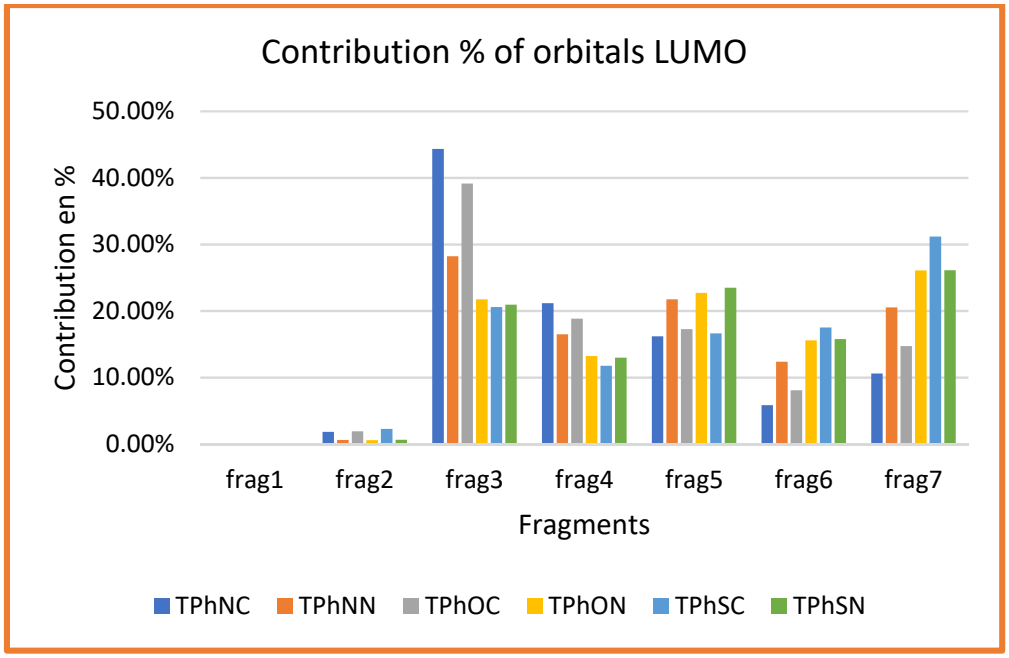

(**a**)

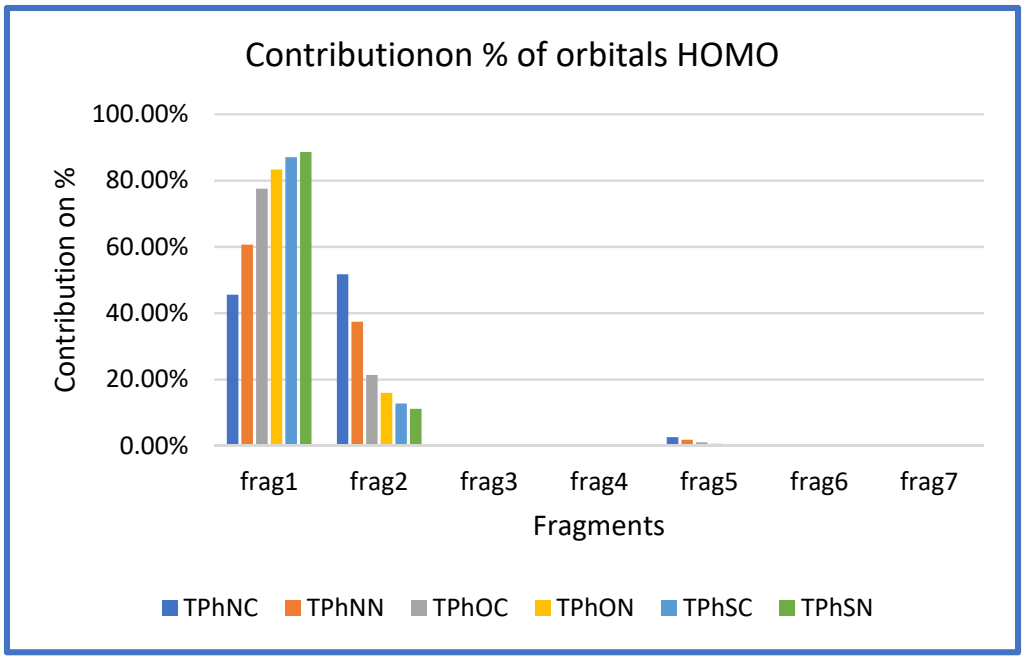

(**b**)

Figure 5. (**a**) Contribution of molecular LUMO orbitals of different fragments for the studied dyes. (**b**) Contribution of molecular HOMO orbitals of different fragments for the studied dyes.

3.3. Photovoltaic Properties

3.3.1. Driving Force

The theoretical background for the photovoltaic parameters is provided in the supplementary file. The ΔG^{inject} are negative values for the studied dyes, and the absolute values of (ΔG^{inject}) are above 0.2 eV. This indicates that the process is spontaneous and favors the introduction of electrons into the conduction band of the semiconductor TiO_2

during stimulation of the dye's excited state [50–52]. Table 3a shows that the injection drive ΔG^{inject} of the dyes decreases in the order of TPhNN > TPhON > TPhSN > TPhNC > TPhOC > TPhSC for the triphenyl-based donor dyes, but when the donor is biphenyl amine, the injection drive ΔG^{inject} of the dyes decreases in the order of 2PhNN > 2PhNC > 2PhSN > 2PhOC > 2PhOC > 2PhSC (Table 3b).

Table 3. a: The calculated redox potential of the ground state stable (E_{ox}^{dye} *in eV*), oxidation potential of the dye (E_{ox}^{dye*} *in eV*), *absorption energy* (E_{00} *in eV*), free energy change for electron injection (ΔG^{inj} *in eV*), *regeneration energy* (ΔG^{reg} *in eV*), *and recombination energy* (ΔG^{rec} *in eV*) *for dye-based triphenylamine.* **b**: The calculated redox potential of the ground state stable (E_{ox}^{dye} *in eV*), oxidation potential of the dye (E_{ox}^{dye*} *in eV*), *absorption energy* (E_{00} *in eV*), free energy change for electron injection (ΔG^{inj} *in eV*), *regeneration energy* (ΔG^{reg} *in eV*), *and recombination energy* (ΔG^{rec} in eV) for dye-based diphenylamine.

(a)

Dyes	E_{ox}^{dye}	E_{00}	E_{ox}^{dye*}	ΔG^{inj}	ΔG^{reg}	ΔG^{rec}
TPhNC	4.76	3.22	1.54	−2.46	0.04	−0.76
TPhOC	4.88	3.23	1.65	−2.35	−0.08	−0.88
TPhSC	4.72	3.21	1.51	−2.49	0.08	−0.72
TPhNN	4.61	2.2	2.41	−1.59	0.19	−0.61
TPhON	4.67	2.86	1.81	−2.19	0.13	−0.67
TPhSN	4.72	3.04	1.68	−2.32	0.08	−0.72

(b)

Dyes	E_{ox}^{dye}	E_{00}	E_{ox}^{dye*}	ΔG^{inj}	ΔG^{reg}	ΔG^{rec}
2PhNC	4.92	3.21	1.71	−2.29	−0.12	−0.92
2PhOC	4.8	3.23	1.57	−2.43	0.00	−0.80
2PhSC	4.64	3.23	1.41	−2.59	0.16	−0.64
2PhNN	4.71	2.43	2.28	−1.72	0.09	−0.71
2PhON	4.88	3.18	1.70	−2.30	−0.08	−0.88
2PhSN	4.97	3.33	1.64	−2.36	−0.17	−0.97

Implying that TPhSC, TPhOC, and 2PhOC, the absolute values of ($|\Delta G^{inject}|$) than other dyes, which conduced to faster injection. Consequently, such dyes possess large J_{SC} compared to the other examined. The process of unfavorable charge analyzation is also analyzed. The greater the ΔG^{rec} value, the easier the charge recombination [53], and enhancing charge separation and reducing charge recombination are efficient ways to raise photoelectric conversion efficiency [54]. The ΔG^{rec} values are negative for all the dyes, indicating that these processes are thermodynamically favorable. The average value of G for the dyes based on triphenylamine is of the order of −0.72 eV. In contrast, this value is of the order of −0.82 eV for the series whose donor is the diphenylamine, which shows that the second series has a high chance of charge recombination.

Electron transfer from the redox electrolyte is required to renew the dye, which is then reduced at the counter electrode. The calculated values of ΔG^{reg} are listed in Table 3a,b. They show positive values except for the TPhOC, 2PhNC, 2PhON, and 2PhSN, suggesting these dyes must be regenerated by electron transfer from the redox electrolyte and then reduced at the counter electrode. This regeneration was in accordance with the low HOMO level of 2PhSN followed by 2PhNC, 2PhON, and TPhOC relative to the redox electrolyte potential.

3.3.2. Absorption Spectra

The conductor-like polarizable continuum model (C-PCM) level of theory functional associated with the excitation was used to determine the absorption spectra using ex-

citation based on the optimization ground-state geometry in a CH_2Cl_2 solvent by the TD-BHandH/6-31G(d,p) level of theory functional. The pertinent photophysical indexes of twelve dyes are displayed in Figure 6, and their corresponding results are summarized in Table 4a,b. As shown in Figure 6, the absorption exhibits a major electronic absorption band in the visible region. For all of the examined dyes, the highest absorption occurs between 300 and 500 nm. The maxima of the dyes presenting the phenyl give a very important LHE compared to the dyes bridged by the triazine. To maximize the photocurrent response, the LHE of the sensitizer should be as high as possible; this is the case with our compounds with phenyl linkers. The above results confirm and recommend that the structure of these dyes is the best model for a dye-sensitized solar cell system.

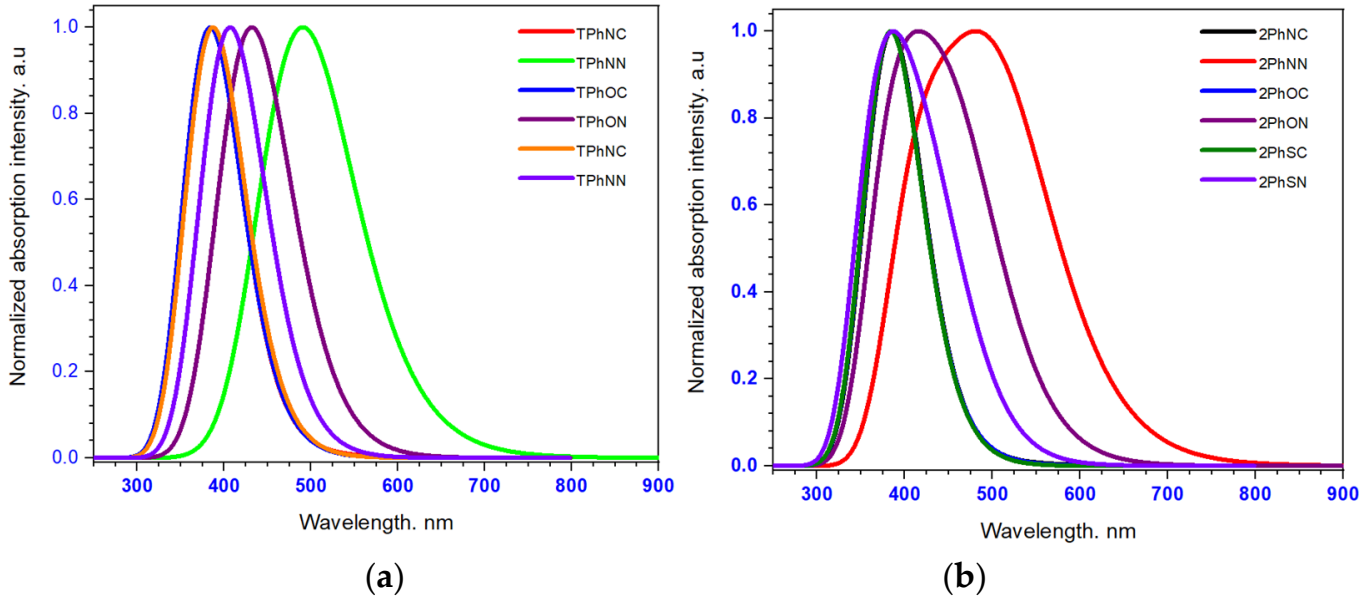

Figure 6. The absorption spectra of dye-based triphenylamine (**a**) diphenylamine (**b**).

Furthermore, the computation in the present manuscript was verified when compared with the optical absorption of bi-anchored sensitizer dyes reported in the literature. As shown in Table 4, the dye-based imidazole exhibits optical absorption from 300–600 nm [55]. In addition, the organic bi-anchored dyes containing triphenylamine/phenothiazine donors, 2-cyanoacrylic acid acceptors, and symmetric double D-π-A with arylamines as donors present almost the same absorption bands in the region (300–550 nm) [56–58].

3.3.3. Dyes@TiO_2 Cluster

The crucial component of DSSC devices is the sensitizer. In order to capture incident photons, it must have strong and widespread optical absorption. In order to decrease charge recombination, the charge transfer must also be unidirectional. As a result, the sensitizers need to be well-conjugated and coplanar. The chelated bidentate binding modes have been kept here among the possible binding modes of the dyes with the $(TiO_2)_9$ cluster (see Figure 5). Numerous dyes with a carboxyl anchor group have been determined to be stable for this bidentate bridging mode [59,60].

Figure 7 shows the structures of dyes@TiO_2 optimized complexes. Bond lengths and torsional angles for these compounds reveal that they mostly remained unaltered during complexation with $(TiO_2)_9$. The length of every dye connection has been reduced from its free form to its complex form.

Table 4. a: Calculated maximum absorption wavelengths (λ_{max}/nm), vertical excitation energy (E_{ex}), oscillator strengths (OS), and major contribution of the dye-based triphenylamine in dichloromethane solution under TD-BHandH/6-31G(d,p) level. **b**: Calculated maximum absorption wavelengths (λ_{max}/nm), vertical excitation energy (E_{ex}), oscillator strengths (OS), and major contribution of the dye-based diphenylamine in dichloromethane solution under TD-BHandH/6-31G (d,p) level.

(**a**)

Dyes	E_{ex} (eV)	λ_{max}(nm)	λ_{exp}(nm) *for Similar Dyes*	*OS*	LHE	*Major Contribution*
TPhNC	2.58	480.12	398/ 400/ 394/ 418/ 388 [55]	0.0188	0.042	H-1→L(17.2), H→L(67.6)
	2.85	434.52		0.0114	0.025	H-1→L+1(15.1), H→+1(68.3)
	3.22	384.46		2.237	**0.994**	H-4→L(25.1), H-2→L+1(47.78), H-1→L(14.9)
TPhOC	2.89	428.14		0.0784	0.165	H-1→L(29.1), H→L(62.6)
	3.15	392.88		0.0646	0.138	H-1→L+1(23.2), H→L+1(64.1)
	3.23	383.07		2.1484	**0.992**	H-1→L(47.4), H→L(11.1), H→L+1(11.6)
TPhSC	2.93	423.06		0.0567	0.122	H-1→L(27.1), H→L(62.7)
	3.14	393.91		0.1541	0.298	H-1→L+1(22.2), H→L+1(61.9)
	3.21	385.61		1.4887	**0.967**	H-2→L+1(36.3), H→L(25.1), H→L+1(21.8)
TPhNN	2.25	550.1		0.0037	0.008	H→L(65.9)
	2.52	490.78		0.3687	**0.572**	H-1→L+1(12.7), H→L+1(59.1)
	2.96	417.98		0.0102	0.023	H-1→L(62.7), H→L+1(21.9)
TPhON	2.62	473.13		0.0001	0.001	H→L(62.8)
	2.86	432.7		0.5146	**0.694**	H→L+1(53.7), H→L+2(21.3)
	3.11	398.29		0.0191	0.043	H-1→L+1(60.1), H→L+1(30.4)
TPhSN	2.87	445.43		0.0002	0.001	H→L(64.8)
	3.04	407.27		0.3538	**0.557**	H→L+1(56.5), H→L+2(15.8)
	3.2	386.88		0.0084	0.019	H-1→L (62.6), H→L(26.4)

(**b**)

Dyes	E_{ex} (eV)	λ_{max}(nm)	λ_{exp}(nm) *for Similar d=Dyes*	OS	LHE	Major Contribution
2PhNC	2.46	502.88	370/ 427/ 444 [56] 320, 403/322, 422/382, 439 [57]	0.012	0.027	H-1→L(11.9), H→L(68.9)
	2.73	454.14		0.0091	0.02	H→L+1(69.3)
	3.21	385.14		2.2556	**0.994**	H-2→L+1(47.5), H-1→H(15.4)
2PhOC	2.71	456.5		0.0312	0.069	H-1→L(13.7), H→L(68.88)
	2.97	416.95		0.0143	0.032	H-1→L+1(10.93), H→L-1(69.9)
	3.22	383.95		2.2926	**0.994**	H-2→L+1(48.5), H-1→H(15.14)
2PhSC	2.42	511.41		0.004	0.009	H-1→L(13.6), H→L(68,3)
	2.68	461.07		0.3951	0.597	H→L+1(62.2), H→L+2(24.2)
	3.18	389.46		0.4317	**0.629**	H-1→L+1(20.3), H→L+2(52.5), H→L+5(15.4)
2PhNN	2.15	575.16		0.0029	0.006	H→L(68.3)
	2.43	508.68		0.3205	**0.521**	H→L+1(63.1)
	2.96	418.84		0.2632	0.454	H-1→L+1(29.1), H→L+2(56.3), H→L+5(15.9)
2PhON	2.42	511.41		0.004	0.009	H-1→L(13.6), H→L(68.3)
	2.68	461.07		0.03951	0.087	H-1→L+2(62.2), H→L+2(24.2)
	3.18	389.46		0.4317	**0.629**	H-1→L+1(20.3), H→L+2(52.5), H→L+5(15.4)
2TPhSN	2.62	472.86		0.0004	0.001	H-1→L(14.7), H→L(68.2)
	2.88	429.64		0.2779	0.472	H-1→L+1(15.4), H→L+1(62.5)
	3.33	371.23		0.3901	**0.592**	H-1→L+2(21.3), H→L (25.5), H→L+1(38.9)

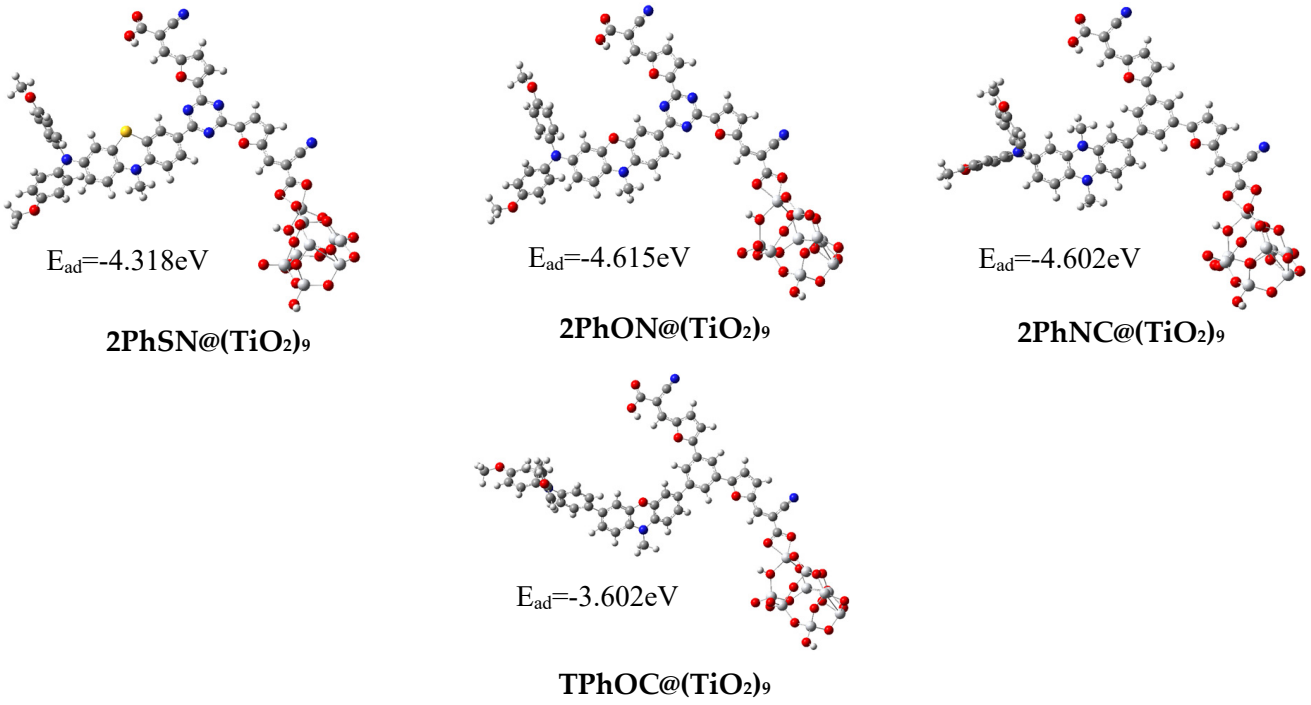

Figure 7. Structure of 2PhSN@$(TiO_2)_9$, 2PhON@$(TiO_2)_9$, 2PhNC@$(TiO_2)_9$, and TPhOC@$(TiO_2)_9$ **complexes**.

The results from the counterpoise correction method, taking into account the basis set superposition errors, are given in Figure 7. The complexation energies of the dyes (Dye@TiO_2) resulting from this method are very low in absolute value. These energy values have an average of −4.248 eV. Thus, BSSE used in this study confirm its importance in calculating the complexation energy as previously reported [61,62].

It is observed that the HOMO orbital energies exhibit a change from the free dyes in terms of stabilization. The behavior of the molecular orbital energies of the dyes isolated and bound to TiO_2 are shown in Figure 8. The energy destabilization is due to the interaction of the dye with the positive Ti(IV) surface ions and the transfer of electrons from the excited-state dye's LUMO to the CB of the TiO_2 cluster. It is noted that the LUMO orbital energies of the free dye are almost on the same level as those of the dyes calculated for the dye-TiO_2 sensitizer, and the destabilization of HOMO upon interaction with the TiO_2 cluster and electron density decreases the HOMO-LUMO energy gaps for adsorbed systems compared to free dyes.

The values of the gap energies of the dyes decrease after complexation with TiO_2. It decreases in the following order: 2PhNC@TiO_2 <2PhSN@TiO_2 <2PhON@TiO_2 <TPhOC@TiO_2. All the complexed dyes show a band lower than the conduction band of TiO_2, whereas the compound 2PhSN@TiO_2 shows a near band of the iodine, which can present a regeneration of the charges compared to the other compounds. The compound 2PhSN@TiO_2 has electronic properties that make it a better colorant.

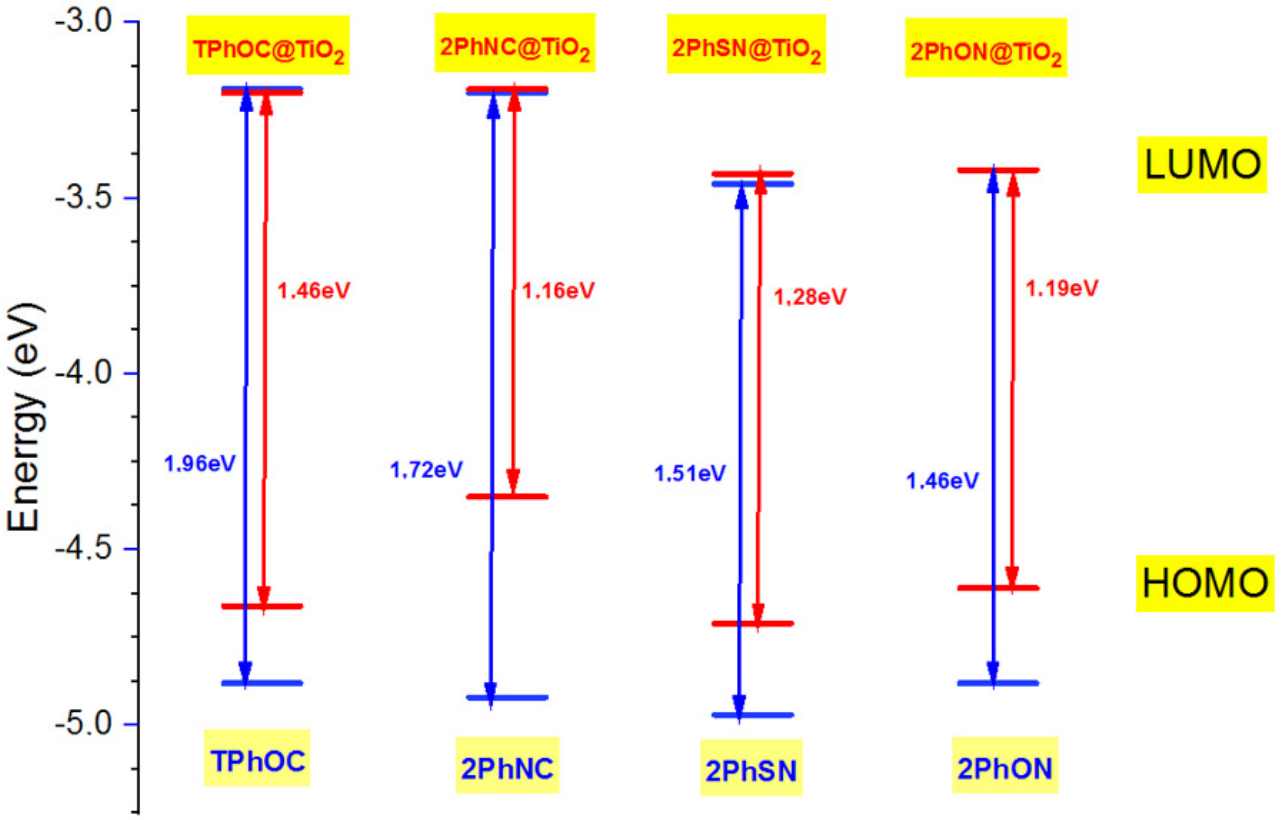

Figure 8. Comparative molecular orbital energies of the isolated and TiO_2-bound studied dyes. The blue and red line represents, respectively, the position of the edge of the conduction and valence band for the isolated and complex dyes (Dye@TiO_2).

4. Conclusions

The DFT and TD-DFT calculations have been performed for the newly designed dyes to analyze and understand organic dyes' electronic structure, absorption, and transport properties. Changing donor (D, D') and π-linkers in the dyes indicate different architectures. The dyes containing triazine π-linker are planar. However, the dyes containing phenyl π-linker are not planar. These results can modify the level of frontier orbitals. The triazine stabilizes the LUMO orbitals while the phenyl destabilizes them. On the other hand, the HOMO orbitals are stabilized for TPhOC, 2PhNC, 2PhSN, and 2PhOC, and allowed regeneration of the electron, compared with other dyes destabilized and do not have the regeneration. For the absorption, the maximum is located between 300–500 nm for the studied dyes. The absorption maxima of the dyes presenting the phenyl give a very important LHE compared to the dyes bridged by the triazine. The adsorption energy increases by modifying the π-linker. The values of the gap energies of the dyes decrease after complexation with TiO_2. It decreases in the following order: 2PhNC@TiO_2 <2PhSN@TiO_2 <2PhON@TiO_2 <TPhOC@TiO_2. Using the counterpoise method when calculating complexation energies can express significant values in absolute terms, which is why it is always essential to consider this method when calculating complexation energies.

Supplementary Materials: The following supporting information can be downloaded at: https://www.mdpi.com/article/10.3390/ma16041611/s1, Figure S1: Optimized structure of the studied dyes. Figure S2: the photovoltaic parameters.

Author Contributions: S.M.B. Conceptualization, Data curation, Formal analysis, Investigation, Writing—review & editing; A.A. Data curation, Formal analysis, Investigation, Writing—review & editing; M.H. Investigation, Resources, Writing—review & editing; F.A.M.A.-Z. Investigation, Funding acquisition, Project administration, —review & editing; M.E.M.Z. Investigation, Writing—review & editing; R.M.E.-S. Concep-

tualization, Investigation, Funding acquisition, Resources, Writing—review & editing. All authors have read and agreed to the published version of the manuscript.

Funding: Deanship of Scientific Research at King Khalid University, under grant number RGP.1/252/43.

Data Availability Statement: All data are presented in the article and Supplementary Material.

Acknowledgments: The authors extend their appreciation to the Deanship of Scientific Research at King Khalid University for funding this work through Small Groups. (Project under grant number (RGP.1/252/43)). The authors are also grateful to the HPCC (Aziz supercomputer) for the resources.

Conflicts of Interest: The authors declare no conflict of interest.

References

1. Kafafy, H.; Wu, H.; Peng, M.; Hu, H.; Yan, K.; El-Shishtawy, R.M.; Zou, D. Steric and Solvent Effect in Dye-Sensitized Solar Cells Utilizing Phenothiazine-Based Dyes. *Int. J. Photoenergy* **2014**, *2014*, 548914. [CrossRef]
2. Yang, C.; Song, P.; El-Shishtawy, R.M.; Ma, F.; Li, Y. Photovoltaic performance and power conversion efficiency prediction of double fence porphyrins. *Phys. Chem. Chem. Phys.* **2021**, *23*, 27042–27058. [CrossRef] [PubMed]
3. Al-Horaibi, S.A.; Asiri, A.M.; El-Shishtawy, R.M.; Gaikwad, S.T.; Rajbhoj, A.S. Synthesis and characterization of new squaraine dyes with bis-pendent carboxylic groups for dye-sensitized solar cells. *J. Mol. Struct.* **2019**, *1195*, 850–858. [CrossRef]
4. Al-Horaibi, S.A.; Asiri, A.M.; El-Shishtawy, R.M.; Gaikwad, S.T.; Rajbhoj, A.S. Indoline and benzothiazole-based squaraine dye-sensitized solar cells containing bis-pendent sulfonate groups: Synthesis, characterization and solar cell performance. *J. Mol. Struct.* **2019**, *1195*, 591–597. [CrossRef]
5. El-Shishtawy, R.; Decoppet, J.-D.; Al-Zahrani, F.; Zakeeruddin, S.; Grätzel, M. Influence of redox electrolyte on the device performance of phenothiazine based dye sen-sitized solar cells. *New J. Chem.* **2018**, *42*, 9045–9050. [CrossRef]
6. El-Shishtawy, R.M.; Asiri, A.M.; Aziz, S.G.; Elroby, S.A.K. Molecular design of donor-acceptor dyes for efficient dye-sensitized solar cells I: A DFT study. *J. Mol. Model.* **2014**, *20*, 2241. [CrossRef]
7. El-Shishtawy, R. Functional dyes, and some hi-tech applications. *Int. J. Photoenergy* **2009**, *2009*, 434897. [CrossRef]
8. Afolabi, S.; Semire, B.; Idowu, M. Electronic and optical properties' tuning of phenoxa-zine-based D-A2-π-A1 organic dyes for dye-sensitized solar cells. DFT/TDDFT investigations. *Heliyon* **2021**, *7*, e06827. [CrossRef]
9. Sun, C.; Li, Y.; Song, P.; Ma, F. An experimental and theoretical investigation of the elec-tronic structures and photoelectrical properties of ethyl red and carminic acid for DSSC application. *Materials* **2016**, *9*, 813. [CrossRef]
10. Jiang, H.; Wu, Y.; Islam, A.; Wu, M.; Zhang, W.; Shen, C.; Zhang, H.; Li, E.; Tian, H.; Zhu, W.-H. Molecular engineering of quinoxaline-based D–A- π–A organic sensitizers: Taking the merits of a large and rigid auxiliary acceptor. *ACS Appl. Mater. Interfaces* **2018**, *10*, 13635–13644. [CrossRef]
11. Mathew, S.; Yella, A.; Gao, P.; Humphry-Baker, R.; Curchod, B.F.E.; Ashari-Astani, N.; Tavernelli, I.; Rothlisberger, U.; Nazeeruddin, K.; Graetzel, M. Dyesensitized solar cells with 13% efficiency achieved through the molecular engineering of porphyrin sensitizers. *Nat. Chem.* **2014**, *6*, 242–247. [CrossRef] [PubMed]
12. Al-Ghamdi, S.; Al-Ghamdi, H.; El-Shishtawy, R.; Asiri, A. Advances in phenothi-azine and phenoxazine-based electron donors for organic dye-sensitized solar cells. *Dye. Pigment.* **2021**, *194*, 109638. [CrossRef]
13. Bifari, E.N.; El-Shishtawy, R.M.; Bouzzine, S.M.; Fadili, D.; Hamidi, M. Synthesis, photophysical, electrochemical and computational investigation of dimethine and trimethine cyanine-based dyes. *J. Photochem. Photobiol. A Chem.* **2022**, *433*, 114189. [CrossRef]
14. Nhari, L.; El-Shishtawy, R.; Bouzzine, S.; Hamidi, M.; Asiri, A. Phenothiazine-based dyes containing imidazole with π-linkers of benzene, furan and thiophene: Synthe-sis, photophysical, electrochemical and computational investigation. *J. Mol. Struct.* **2022**, *1251*, 131959. [CrossRef]
15. Stathatos, E. Dye sensitized solar cells as an alternative approach to the conventional pho-tovoltaic technology based on silicon-Recent developments in the field and large scale applications. In *Solar Cells: Dye-Sensitized Devices*; IntechOpen: London, UK, 2011; pp. 471–492.
16. O'regan, B.; Grätzel, M. A low-cost, high-efficiency solar cell based on dye-sensitized col-loidal TiO_2 films. *Nature* **1991**, *353*, 737–740. [CrossRef]
17. Akhtaruzzaman, M.; Selvanathan, V.; Hassan, A. Dye-sensitized solar cells. In *Comprehensive Guide on Organic and Inorganic Solar Cells*; Elsevier: Amsterdam, The Netherlands, 2022; pp. 195–244.
18. El Mzioui, S.; Bouzzine, S.M.; Bourass, M.; Bennani, M.N.; Hamidi, M. A theoretical investigation of the optoelectronic performance of some new carbazole dyes. *J. Comput. Electron.* **2019**, *18*, 951–961. [CrossRef]
19. Damaceanu, M.-D.; Mihaila, M.; Constantin, C.-P.; Chisca, S.; Serban, B.-C.; Diaconu, C.; Buiu, O.; Pavelescu, E.; Kusko, M. A new sensitizer containing dihexyloxy-substituted tri-phenylamine as donor and a binary conjugated spacer for dye-sensitized solar cells. *RSC Adv.* **2015**, *5*, 53687–53699. [CrossRef]
20. El Mzioui, S.; Bouzzine, S.M.; Sidir, I.; Bouachrine, M.; Bennani, M.N.; Bourass, M.; Hamidi, M. Theoretical investigation on π-spacer effect of the D–π–A organic dyes for dye-sensitized solar cell applications: A DFT and TD-BHandH study. *J. Mol. Model.* **2019**, *25*, 92. [CrossRef]

21. Sun, Z.-D.; He, M.; Chaitanya, K.; Ju, X.-H. Theoretical studies on DA-π-A and D-(A-π-A) 2 dyes with thiophene-based acceptor for high performance p-type dye-sensitized solar cells. *Mater. Chem. Phys.* **2020**, *248*, 122943. [CrossRef]
22. Constantin, C.-P.; Damaceanu, M.-D.; Mihaila, M.; Kusko, M. Open-Circuit Voltage Degra-dation by Dye Mulliken Electronegativity in Multi-Anchor Organic Dye-Based Dye-Sensitized Solar Cells. *ACS Appl. Energy Mater.* **2022**, *5*, 7600–7616. [CrossRef]
23. Mahmoud, S.E.; Fadda, A.; Abdel-Latif, E.; Elmorsy, M. Synthesis of Novel Triphenyl-amine-Based Organic Dyes with Dual Anchors for Efficient Dye-Sensitized Solar Cells. *Nanoscale Res. Lett.* **2022**, *171*, 71. [CrossRef] [PubMed]
24. Shi, X.; Zhao, D.; Wang, L.; Li, Y. A DFT study of influence of dichloromethane solvent and electric field on light absorption and electronic properties of two Quinoxaline-based solar cells. *Optik* **2020**, *219*, 165030. [CrossRef]
25. Gauthier, S.; Guen, F.R.-L.; Wojcik, L.; Le Poul, N.; Planchat, A.; Pellegrin, Y.; Level, P.G.; Szuwarski, N.; Boujtita, M.; Jacquemin, D.; et al. Comparative studies of new pyranylidene-based sensitizers bearing single or double anchoring groups for dye-sensitized solar cells. *Sol. Energy* **2020**, *205*, 310–319. [CrossRef]
26. Desta, M.; Chaurasia, S.; Lin, J. Reversed Y-shape di-anchoring sensitizers for dye sen-sitized solar cells based on benzimidazole core. *Dye. Pigment.* **2017**, *140*, 441–451. [CrossRef]
27. Wang, Z.; Chen, Q.; Zou, Y.; Chen, J.; Luo, Y.; Liu, Y.; Ding, S.; Cai, P.; Yuan, J.; Liang, M. Judi-cious design of L (D-π-A) 2 type di-anchoring organic sensitizers for highly efficient dye-sensitized solar cells: Effect of the donor-linking bridges on functional properties. *Dye. Pigment.* **2021**, *187*, 109134. [CrossRef]
28. Park, S.S.; Won, Y.S.; Choi, Y.C.; Kim, J.H. Molecular Design of Organic Dyes with Double Electron Acceptor for Dye-Sensitized Solar Cell. *Energy Fuels* **2009**, *23*, 3732–3736. [CrossRef]
29. Abbotto, A.; Leandri, V.; Manfredi, N.; De Angelis, F.; Pastore, M.; Yum, J.-H.; Nazeeruddin, M.K.; Grätzel, M. Bis-Donor-Bis-Acceptor Tribranched Organic Sensitizers for Dye-Sensitized Solar Cells. *Eur. J. Org. Chem.* **2011**, *2011*, 6195–6205. [CrossRef]
30. Sirohi, R.; Kim, D.H.; Yu, S.-C.; Lee, S.H. Novel di-anchoring dye for DSSC by bridging of two mono anchoring dye molecules: A conformational approach to reduce aggregation. *Dye. Pigment.* **2012**, *92*, 1132–1137. [CrossRef]
31. Grisorio, R.; De Marco, L.; Allegretta, G.; Giannuzzi, R.; Suranna, G.P.; Manca, M.; Mastrorilli, P.; Gigli, G. Anchoring stability and photovoltaic properties of new D(-π-A)2 dyes for dye-sensitized solar cell applications. *Dye. Pigment.* **2013**, *98*, 221–231. [CrossRef]
32. Frisch, M.J.; Trucks, G.W.; Schlegel, H.B.; Scuseria, G.E.; Robb, M.A.; Cheeseman, J.R.; Scalmani, G.; Barone, V.; Mennucci, B.; Petersson, G.A.; et al. Sonnenber. In *Gaussian 09*; Gaussian Inc.: Wallingford, CT, USA, 2009.
33. Fadili, D.; Bouzzine, S.M.; Hamidi, M. Study of the structural and optoelectronic properties of dye solar cells based on phosphonic acid anchoring by DFT functionals. *New J. Chem.* **2020**, *45*, 2723–2733. [CrossRef]
34. Fadili, D.; Bouzzine, S.M.; Hamidi, M. Effects of adding cyanovinyl moiety on the photovoltaic DSSCs phosphonic acid based cells. *J. Comput. Electron.* **2020**, *19*, 1629–1644. [CrossRef]
35. Cavanagh, M.M.; Weyand, C.M.; Goronzy, J.J. Chronic inflammation and aging: DNA damage tips the balance. *Curr. Opin. Immunol.* **2012**, *24*, 488–493. [CrossRef] [PubMed]
36. Malmir, H.; Vosoughi, N. On-line reactivity calculation using Lagrange method. *Ann. Nucl. Energy* **2013**, *62*, 463–467. [CrossRef]
37. Becke, A.D. A new mixing of Hartree–Fock and local density-functional theories. *J. Chem. Phys.* **1993**, *98*, 1372–1377. [CrossRef]
38. Schuchardt, K.L.; Didier, B.T.; Elsethagen, T.; Sun, L.; Gurumoorthi, V.; Chase, J.; Li, J.; Windus, T.L. Basis Set Exchange: A Community Database for Computational Sciences. *J. Chem. Inf. Model.* **2007**, *47*, 1045–1052. [CrossRef] [PubMed]
39. Pritchard, B.P.; Altarawy, D.; Didier, B.T.; Gibson, T.D.; Windus, T.L. New Basis Set Exchange: An Open, Up-to-Date Resource for the Molecular Sciences Community. *J. Chem. Inf. Model.* **2019**, *59*, 4814–4820. [CrossRef] [PubMed]
40. Feller, D. The role of databases in support of computational chemistry calculations. *J. Comput. Chem.* **1996**, *17*, 1571–1586. [CrossRef]
41. Fadili, D.; Fahim, Z.M.E.; Bouzzine, S.M.; Hamidi, M. Improved photovoltaic performance of phosphonic acid-based sensitized solar cells via an electron-withdrawing moiety: A density of functional theory study. *Int. J. Quantum Chem.* **2020**, *121*, e26431. [CrossRef]
42. Tomasi, J.; Mennucci, B.; Cammi, R. Quantum Mechanical Continuum Solvation Models. *Chem. Rev.* **2005**, *105*, 2999–3094. [CrossRef]
43. Chandra, A.; Bhanuprakash, K. An ab initio study with counterpoise correction of ethylene dimer- and trimer-cations. *J. Mol. Struct. THEOCHEM* **1987**, *151*, 149–155. [CrossRef]
44. Davidson, E.R.; Chakravorty, S.J. Chakravorty. A possible definition of basis set su-perposition error. *Chem. Phys. Lett.* **1994**, *217*, 48–54. [CrossRef]
45. Kestner, N.R.; Combariza, J.E. Basis set superposition errors: Theory and practice. *Rev. Comput. Chem.* **1999**, *13*, 99–126.
46. Hachi, M.; Slimi, A.; Fitri, A.; Benjelloun, A.T.; El Khattabi, S.; Benzakour, M.; Mcharfi, M.; Khenfouch, M.; Zorkani, I.; Bouachrine, M. Theoretical design and characterization of D-A1-A based organic dyes for efficient DSSC by altering promising acceptor (A1) moiety. *J. Photochem. Photobiol. A Chem.* **2021**, *407*, 113048. [CrossRef]
47. Chen, X.; Jia, C.; Wan, Z.; Zhang, J.; Yao, X. Theoretical investigation of phenothiazine–triphenylamine-based organic dyes with different π spacers for dye-sensitized solar cells. *Spectrochim. Acta Part A Mol. Biomol. Spectrosc.* **2014**, *123*, 282–289. [CrossRef]
48. Chitpakdee, C.; Jungsuttiwong, S.; Sudyoadsuk, T.; Promarak, V.; Kungwan, N.; Namuangruk, S. Modulation of π-spacer of carbazole-carbazole based organic dyes toward high efficient dye-sensitized solar cells. *Spectrochim. Acta Part A Mol. Biomol. Spectrosc.* **2017**, *174*, 7–16. [CrossRef]

49. Fahim, Z.; Hamidi, M.; Bouzzine, S.; Hamidi, M. Investigations of the bridged thi-ophene derivative effect on the performance of N, N-diethylaniline-based compounds for organic photovoltaic cells. *Orbital Electron. J. Chem.* **2010**, *10*, 84–91.
50. Grätzel, M. Recent Advances in Sensitized Mesoscopic Solar Cells. *Accounts Chem. Res.* **2009**, *42*, 1788–1798. [CrossRef]
51. Pastore, M.; Fantacci, S.; De Angelis, F. Ab Initio Determination of Ground and Excited State Oxidation Potentials of Organic Chromophores for Dye-Sensitized Solar Cells. *J. Phys. Chem. C* **2010**, *114*, 22742–22750. [CrossRef]
52. Assyry, A.; Jdaa, R.; Benali, B.; Addou, M.; Zarrouk, A. Optical and photovoltaic properties of new quinoxalin-2(1H)-one-based D-A organic dyes for efficient dye-sensitized solar cell using DFT. *J. Mater. Environ. Sci.* **2015**, *6*, 2612–2623.
53. Kong, L.; He, M.; Yan, W.; Zhang, C.; Ju, X. Theoretical studies on triaryamine-based p-type D-D-π-A sensitizer. *J. Chin. Chem. Soc.* **2019**, *66*, 1257–1262. [CrossRef]
54. Kong, L.-X.; Zhang, C.-S.; Xia, Q.-Y.; Ju, X.-H. Theoretical study of the effect of π-linkers on triarylamine-based *p*-type D-π-A sensitiser. *Mol. Simul.* **2019**, *46*, 128–135. [CrossRef]
55. Yen, Y.-S.; Ni, J.-S.; Lin, T.-Y.; Hung, W.-I.; Lin, J.; Yeh, M.-C.P. Imidazole-Based Sensitizers Containing Double Anchors for Dye-Sensitized Solar Cells. *Eur. J. Org. Chem.* **2015**, *2015*, 7367–7377. [CrossRef]
56. Bodedla, G.B.; Thomas, K.; Fan, M.-S.; Ho, K.-C. Bi-Anchoring Organic Dyes That Contain Benzimidazole Branches for Dye-Sensitized Solar Cells: Effects of π Spacer and Peripheral Donor Groups. Chem. *Asian J.* **2016**, *11*, 2564–2577. [CrossRef]
57. Hong, Y.; Liao, J.-Y.; Fu, J.; Kuang, D.-B.; Meier, H.; Su, C.-Y.; Cao, D. Performance of Dye-Sensitized Solar Cells Based on Novel Sensitizers Bearing Asymmetric Double D- π- A Chains with Arylamines as Donors. *Dye. Pigment.* **2012**, *94*, 481–489. [CrossRef]
58. Kumar, D.; Wong, K.-T. Organic Dianchor Dyes for Dye-Sensitized Solar Cells. Mater. *Today Energy* **2017**, *5*, 243–279. [CrossRef]
59. Xia, H.-Q.; Wang, J.; Bai, F.-Q.; Zhang, H.-X. Theoretical studies of electronic and optical properties of the triphenylamine-based organic dyes with diketopyrrolopyrrole chromo-phore. *Dye. Pigment.* **2015**, *113*, 87–95. [CrossRef]
60. Al-Marhabi, A.R.; El-Shishtawy, R.M.; Bouzzine, S.M.; Hamidi, M.; Al-Ghamdi, H.A.; Al-Footy, K.O. D-D-π-A-π-A-based quinoxaline dyes incorporating phenothiazine, phenoxazine and carbazole as electron donors: Synthesis, photophysical, electrochemical, and computational investigation. *J. Photochem. Photobiol. A Chem.* **2023**, *436*, 114389. [CrossRef]
61. Galano, A.; Alvarez–Idaboy, J.R. A new approach to counterpoise correction to BSSE. *J. Comput. Chem.* **2006**, *27*, 1203–1210. [CrossRef]
62. Salvador, P.; Paizs, B.; Duran, M.; Suhai, S. On the effect of the BSSE on intermolecular potential energy sur-faces. Comparison of a priori and a posteriori BSSE correction schemes. *J. Comput. Chem.* **2001**, *22*, 765–786. [CrossRef]